Pharmaceutical Research, Vol. 25, No. 1, January 2008 (© 2007)
DOI: 10.1007/s11095-007-9350-0

Research Paper

Characterization of Solid Maltose Microneedles and their Use for Transdermal Delivery

Chandra Sekhar Kolli[1] and Ajay K. Banga[1,2]

Received March 16, 2007; accepted May 15, 2007; published online June 28, 2007

Purpose. To characterize solid maltose microneedles and assess their ability to increase transdermal drug delivery.

Materials and Methods. Microneedles and microchannels were characterized using methylene blue staining and scanning electron microscopy. Diffusion pattern of calcein was observed using confocal scanning laser microscopy. Transepidermal water loss (TEWL) measurements were made to study the skin barrier recovery after treatment. Uniformity in calcein uptake by the pores was characterized and percutaneous penetration of nicardipine hydrochloride (NH) was studied *in vitro* and *in vivo* across hairless rat skin.

Results. Microneedles were measured to be 508.46 ± 9.32 μm long with a radius of curvature of 3 μm at the tip. They penetrated the skin while creating microchannels measuring about 55.42 ± 8.66 μm in diameter. Microchannels were visualized by methylene blue staining. Pretreatment with microneedles resulted in the migration of calcein into the microchannels. TEWL increased after pretreatment and uptake of calcein by the pores was uniform as measured by the pore permeability index values. NH *in vitro* transport across skin increased significantly after pretreatment (flux 7.05 μg/cm^2/h) as compared to the untreated skin (flux 1.72 μg/cm^2/h) and the enhanced delivery was also demonstrated *in vivo* in hairless rats.

Conclusion. Maltose microneedles were characterized and shown to create microchannels in the skin, which were also characterized and shown to improve the transdermal delivery of NH.

KEY WORDS: confocal microscopy; microneedles; nicardipine hydrochloride; transdermal delivery; transepidermal water loss.

INTRODUCTION

The skin is an easily accessible and an attractive organ for the delivery of therapeutic molecules but delivery is often limited due to its extremely low permeability. The outermost lipophilic layer of the skin, composed of dead tissue called the stratum corneum (SC), which is about 10–20 μm in thickness (1), constitutes a major obstacle and severely limits the delivery of molecules. Researchers off late have explored a variety of methods to breach this barrier including use of penetration enhancers, lasers, electrical energy, ultrasound, radio frequency, and thermal energy and various approaches followed for this purpose have been extensively reviewed (2,3). Amongst these microneedles appear to be a promising approach to physically disrupt the SC and circumvent the barrier.

The usage of micron-sized microneedles for transdermal drug delivery is an approach that is cost effective, minimally invasive and can enhance delivery across skin by disrupting the SC thereby creating microscopic channels for the drug transport (4). These microneedles are long enough to penetrate SC, but too short to reach and stimulate the nerves that perceive pain. Further, it is rapid and convenient and drug molecules can be placed at a desired depth in skin by choosing appropriate needle length.

Microneedles typically used are made of a variety of substances like metal, silicon, titanium or glass (5). The initial development of microneedle to create transport pathways through the SC involved usage of silicon. However, these are made by complex dry and wet etch technologies, which need dedicated and costly clean room facilities. Also, if silicon or metal needles break off in the skin, then it would result in possible complications. In contrast, microneedles made of sugars like maltose, such as what we used, will dissolve instantly in the skin to create microchannels. Furthermore, they can be made by a simple and cheap micromoulding technique. Therefore recent focus has been towards biodegradable microneedles that are inexpensive and biocompatible (6–8).

[1] Department of Pharmaceutical Sciences, College of Pharmacy and Health Sciences, Mercer University, 3001 Mercer University Drive, Atlanta, Georgia 30341, USA.
[2] To whom correspondence should be addressed. (e-mail: banga_ak@mercer.edu)

ABBREVIATIONS: NH, Nicardipine hydrochloride; PPI, Pore Permeability Index; SC, Stratum corneum; SEM, Scanning electron microscope; TEWL, Transepidermal water loss.

Maltose a carbohydrate and a GRAS substance was chosen for the manufacture of microneedles, because it has been used for long as a sweetener, bulking agent and as an excipient in pharmaceutical formulations. It is also used as an additive in parenteral formulations. Its crystalline form makes it a candidate for fabrication of microneedles. The added feature of these microneedles is that they are designed to break into the skin, dissolve and disappear rapidly while creating the microscale conduits. Unlike the polymeric needles that are biodegradable and remain in the skin for a period of time, these are readily soluble and dissolve within minutes.

Nicardipine hydrochloride (NH) [(±)-2-(benzyl-methyl amino) ethyl methyl 1,4-dihydro-2,6-dimethyl-4-(m-nitrophenyl)-3,5-pyridinedicarboxylate monohydrochloride], a dihydropyridine derivative, is a calcium channel blocker used in the treatment of hypertension. It was selected as model drug for this investigation because it undergoes rapid and extensive hepatic first pass metabolism, resulting in a low oral bioavailability of about 15–40% (9). In addition, it has a short elimination half-life (10) and these factors make NH a candidate for transdermal drug delivery. Diez *et al.* (11) studied the transdermal permeation of series of calcium channel blockers to determine the permeation parameters and reported that nicardipine showed a higher mean transdermal penetration value than the other dihydropyridines and hence suggested that nicardipine would be the most suitable candidate for formulation in a transdermal delivery system.

The present work focuses on the characterization of solid microneedles fabricated using maltose as a substrate employing micromoulding technology in brief and assess their ability to disrupt the SC and increase drug transport across rat skin.

MATERIALS AND METHODS

Materials

Nicardipine hydrochloride and ethanol were purchased from Sigma (St. Louis, MO, USA). Calcein (FLUORESOFT® 0.35% solution) was obtained from Holles labs, Inc, (Cohasset, MA, USA). Other chemicals were obtained from Fisher Scientific (Pittsburgh, PA, USA). Hairless rats were obtained from Charles River (Wilmington, MA, USA) and were housed in the animal facility at Mercer University until used.

Methods

Fabrication

Microneedles designed and supplied by Texmac Inc (USA) employed maltose, a disaccharide, as base material for the manufacture of microneedles. Mould-based fabrication methods have been employed for the manufacture that can lead to mass production. By adapting micromoulding technology, three-dimensional arrays of sharp-tipped and solid tetrahedron shaped microneedles were made. To fabricate micromoulds, an etching process is used to cast the inverse shape of the microneedles. The length of micromoulds ranged from 200 μm to 2 mm depending on the length of microneedles desired. The procedure to manufacture these microneedles was reported elsewhere (12). These needles are designed for manual insertion into the skin while applying a pressure of about 0.35–0.5 N. Unless otherwise specified, 500 μm microneedles were used for the experiments.

Scanning Electron Microscopy

Freshly excised full thickness hairless rat skin was treated with microneedles and fixed for scanning electron microscopy using 2.5% glutaraldehyde and washed; excess water was blotted and later skin samples were dried in vacuum to about 100 Torr. They were then mounted on a metal stub using double-sided carbon sticky tape and sputter coated using Hummer VI Sputtering System (Anatech, USA) with Au/Pd target. Skin samples were examined using field emission scanning electron microscope (Hitachi, S4100) integrated with a critical dimension measurement system. Primary beam accelerating voltage was 15 kV and secondary ion images were collected. Similar procedure was followed but without fixing step for obtaining SEM images for microneedles.

For the calculation of radius of curvature, X 3500 SEM image that show the tip of a needle was collected and transferred into Image-Pro image analysis software (Media Cybernetics, Inc., USA). The image was then calibrated for the magnification and the radius of the tip was determined using the measurement tools.

Dye Binding Studies for Visualization of Microchannels

Full thickness hairless rat skin was pretreated with microneedles. Methylene blue staining involved a 5 min surface application of few drops of methylene blue solution on the treated skin followed by removal of excessive stain using sterile saline swabs and later with alcohol swabs. Stained skin was visualized using a video microscope system (Hi-Scope KH2200, Hirox Co., Japan). In some studies, skin sites were photographed using a digital camera (Canon Inc., USA).

Confocal Microscopy Studies

We have used confocal microscopy to visualize the distribution of calcein in the skin pretreated with microneedles. A computerized Zeiss confocal laser microscope LSM410 (Goettinger, Germany) with ×10 objective was used to obtain the fluorescent images. Before examination, hairless rat skin was pretreated with single array of microneedles and the treated skin was covered using a 1 cm^2 liquid reservoir patch. Patch was filled with calcein and allowed to stand for 5 min in darkness. It was then removed; excess calcein was thoroughly wiped using saline and alcohol swabs. The skin samples were later placed on a microscope slide with phosphate-buffered saline and glycerol (80:20) and then scanned using the confocal microscope. While obtaining fluorescent images, all samples were excited at 488 nm and X–Z sectioning has been used to determine the permeation pathways.

Assessment of Barrier Perturbation by TEWL Measurements

The objective of this study was to examine the barrier integrity of hairless rat skin after poration with microneedles as assessed with TEWL.

The study was conducted in ambient conditions (room temperature, relative humidity). The barrier function of SC was evaluated by measuring TEWL using a Cyberderm evaporimeter (Cortex Technology, Denmark). The probe was held on the skin till a stable reading was obtained (40 s) and measurements were recorded for the next 20 s. The data was collected and processed using Desylab software (Cortex Technology, Denmark). Ten minutes after pretreatment with microneedles, TEWL over the treated locations was measured. The measurements were performed according to guidelines (13) and recorded in triplicate. To examine if the barrier perturbation was due to cardboard base of the microneedle holder, skin was treated with just the base with all microneedles removed from the array and normal skin served as a control. In a separate experiment, we have studied the effect of number of pores created on the skin on the TEWL values using 26 G hypodermic needle and increasing arrays of maltose microneedles. Also, TEWL was measured following tape stripping to add a positive control that represents a condition where there is total disruption of stratum corneum.

In the absence of visual damage, an assessment of methylene dye penetration was carried out as mentioned in earlier section on the control and treated tissues to determine if the TEWL values obtained as the result of increased skin permeability are due to physical damage by means other than microneedles. In such case, the dye when applied to the skin surface rapidly penetrates and stains the underlying tissue exposing also the other damaged areas of SC.

Characterization of Pore Uniformity

This study investigates using Fluoropore software, an image analysis tool, the relative skin permeability following treatment with microneedles and creation of microchannels. It also gives an estimate of relative flux values of individual pores.

Calcein solution was applied to the skin portion treated with microneedles for one minute, using a liquid reservoir patch. Upon removal, the site is wiped off using saline and alcohol swabs. A fluorescent image was taken that shows the two-dimensional distribution of fluorescent intensity in and around each pore created by microneedle. The imaging system comprised of a digital camera (Canon, USA) fitted with a macro-lens attached in front with a 525 nm long pass filter. A fiber-optic ring light surrounds the lens and coupled with a tungsten–halogen source with a 440–520 nm filter installed. A hollow aluminum cone is attached to the ring-light that extends to the image plane of the macro lens. Over all, the design provides a flat field illumination of the field-of-view and excludes all the ambient light. The image data is processed to produce a Pore Permeability Index (PPI), a number representative of calcein flux into the underlying tissue, for each pore.

Microneedle Mediated In Vitro Transdermal Delivery of NH

In vitro permeation studies were carried out with jacketed Franz diffusion cells having a 0.64 cm^2 diffusion area (PermeGear, Bethlehem, PA, USA). Donor solution was composed of 500 μl of 10 mg/ml NH in pH 4.0 citrate buffer containing 20% ethanol. The receptor compartments were filled with 5 ml of citrate buffer pH 4.0 containing 10% of ethanol. Temperature was maintained at 37°C with the help of a double water circulation jacket surrounding the lower part of the cell. This enabled the skin surface temperature to be maintained at about 32°C.

The microneedle arrays were manually pressed into freshly excised full thickness hairless rat skin. Treated skin was then clamped between the donor and receptor chambers of a vertical diffusion cell with the SC side in contact with the donor solution.

The amount of drug diffused was determined by removing aliquots of 300 μl at various time intervals from the receptor compartments using a syringe and immediately replenishing with the same volume of receptor solution. The samples were stored in a refrigerator until they were analyzed.

In Vivo Studies

Male hairless rats, 10 week old and weighing 326.4 ± 11.8 g, whose right jugular vein was cannulated was anesthetized with an intraperitoneal injection of ketamine (70 mg/kg) and xylazine (10 mg/kg). A blood sample was obtained 15 min before pretreatment with microneedles. The abdominal area was cleaned gently using alcohol swabs and allowed to dry. Maltose microneedles stacked in six parallel layers were inserted manually into the abdominal skin and a custom-made liquid reservoir patch was placed on the treated area. It was filled with 350 μl of NH (10 mg/ml in pH 4.0 citrate buffer containing 20% ethanol) and sealed. Blood samples were collected at predetermined time intervals and plasma was separated. Control study was conducted following the same procedure but without pretreatment with microneedles. Animal experiments were all carried out in accordance with Mercer University IACUC guidelines for animal experiments.

Quantitative Analysis

Nicardipine in plasma samples was analyzed using HPLC. The method was sensitive down to 5 ng/ml levels. Briefly, an aliquot of 200 μl of the plasma was added to a screw-capped glass tube and 100 μl of 0.2 N KOH was added and the solution was mixed well. A 4 ml volume of dichloromethane (containing 20 ng/ml nimodipine as an internal standard) was added as an extracting solvent and shaken at 300 rpm for 15 min. The mixture was centrifuged and organic layer was carefully separated. The extraction was repeated with 3 ml of dichloromethane and pooled organic layers were evaporated to until dry with nitrogen, and then reconstituted with 150 μl of mobile phase. After 30 s of vortex, 60 μl of the sample solution were injected into the HPLC system.

Analysis of NH was performed on an HPLC system (Waters LC Module 1, USA). Samples were eluted on a C18 column (Phenomenex; 25 cm × 4.6 mm; 5 μm) using a mobile phase consisting of phosphate buffer (0.05 M dihydrogen orthophosphate adjusted to pH 6.3 with triethylamine) and acetonitrile (30:70). A flow rate of 1 ml/min was maintained, 60 μl of the sample was spiked onto the column and the detection wavelength was 240 nm.

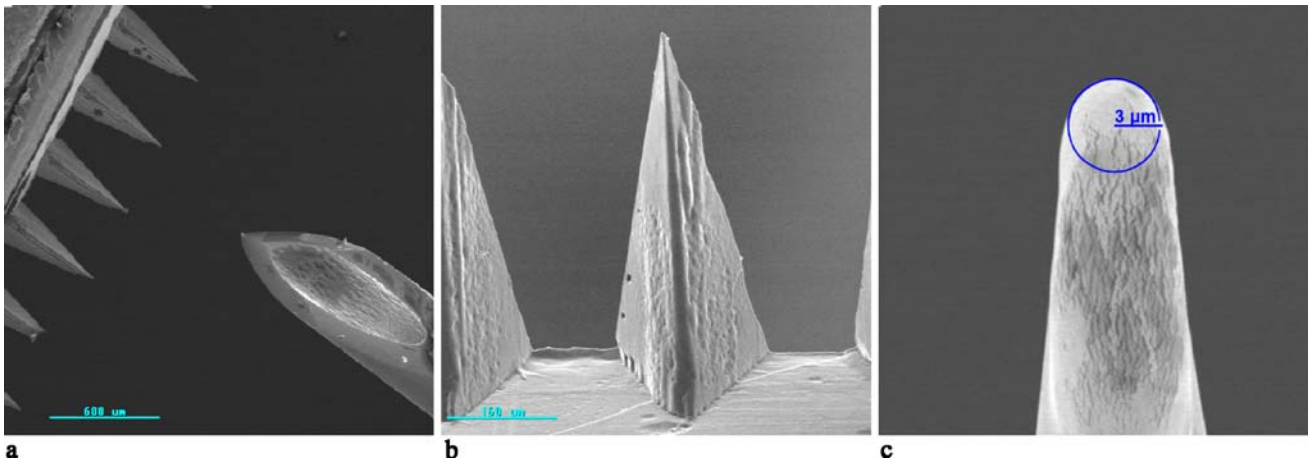

Fig. 1. Scanning electron micrograph image of 500 µm long solid maltose microneedles shown opposite to a tip of a 26 G hypodermic needle (**a**), in an individual array (**b**) and magnified view that show the radius of the tip (**c**).

Data Analysis

All results are presented as means with respective standard deviation. Statistical analysis was composed of analysis of variance. The cumulative amount of drug permeated through a unit area of skin was plotted as a function of time. The *in vitro* steady-state permeation flux was calculated from the slope of the linear portion of the plot.

RESULTS

Fabrication

Microneedle arrays were designed to obtain 27 microneedles each 500 µm tall, per array and number of arrays can be stacked to get desired microneedle density. The standard deviation of needle height within an array or among the arrays is less than 3%.

Scanning Electron Microscopy

Small dimensions of these microneedles can be appreciated from the SEM image presented in Fig. 1a, where 500 µm long maltose microneedles were placed opposite to a tip of a 26 G hypodermic needle. Figure 1b shows the SEM picture of individual microneedle from the array whose height was measured to be 508.46 ± 9.32 µm and length of the equilateral base was 204.62 ± 7.19 µm. Radius of curvature of the tip (Fig. 1c) was calculated to be 3 µm, which indicates that microneedles are sharp and can penetrate the stratum corneum. The microneedles are spaced at a distance of about 150 µm from the adjacent ones within the same array. Figure 2 show the scanning electron micrograph of hairless rat skin that was treated with microneedles and removed after 30 s. Microneedles penetrated the skin by localized disruption of the stratum corneum.

Dye Binding Studies for Visualization of Microchannels

Figure 3a shows the picture full thickness hairless rat skin stained by methylene blue dye following treatment with microneedles stacked in six layers. The areas of the skin breached by microneedles took up the dye whereas the rest of the skin remained impermeable. Picture at higher magnification, Fig. 3b, show that the dye diffuses along the periphery of the microchannels. Distance between microchannels created in the skin within the same array of microneedle was on average 376.38 ± 14.37 µm and between different arrays it was 1071.10 ± 64.92 µm. Skin treated with six single arrays of microneedles stacked together resulted in a pore density of approximately 250 pores per square centimeter.

Confocal Microscopy Studies

The skin sample was imaged and recorded at increasing depths from the skin surface (Fig. 4a–f). The area away from microchannels served as control and it reveals that no dye was imaged in lower epidermal tissue below the control. In contrast, in the region of skin that was pretreated with microneedles, and the stratum corneum is breached; calcein migrated down through the stratum corneum, along the

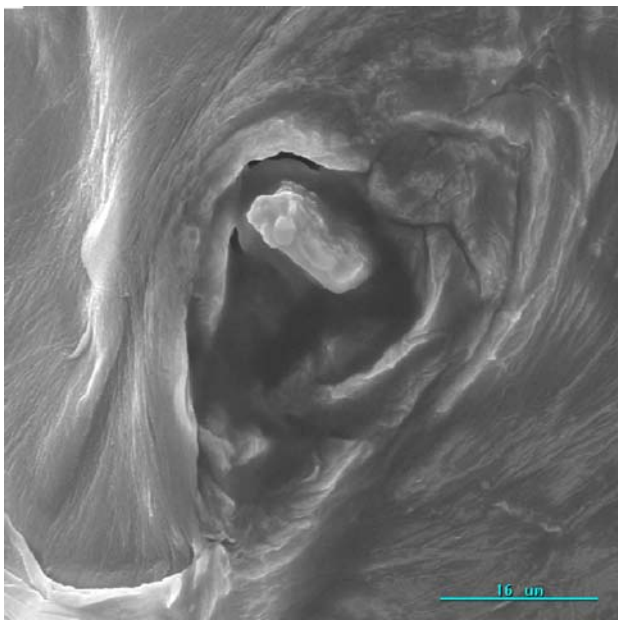

Fig. 2. Scanning electron micrograph image of surface morphology of full thickness hairless rat skin treated with 500 µm maltose microneedles.

microchannels and into the lower epidermal tissue. Hair follicles could not be seen in absence of calcein, but were clearly visible as dark spots scattered throughout the sample in presence of fluorescence from calcein.

Assessment of Barrier Perturbation by TEWL Measurements

As shown in Fig. 5, an increase in TEWL ($g/m^2/h$) was measured as % change from base value (before treatment) immediately following treatment with microneedles. A measurable difference from the baseline is indicative of disruption of the SC and also sites pierced with hypodermic needle showed statistically significantly higher TEWL values. However, there was no significant difference ($P < 0.05$) between the control and TEWL measured at sites treated with the base of microneedle.

Further, it was observed that increasing the number of pores created on the skin using hypodermic needle increased the TEWL values up to a certain limit and later no further increase was noticed. Similar results were seen with increase in number of arrays of microneedle arrays and thereby increasing micropores. TEWL recorded following tape stripping demonstrated significantly higher values (43.5 $g/m^2/h$) as compared to the other treatments.

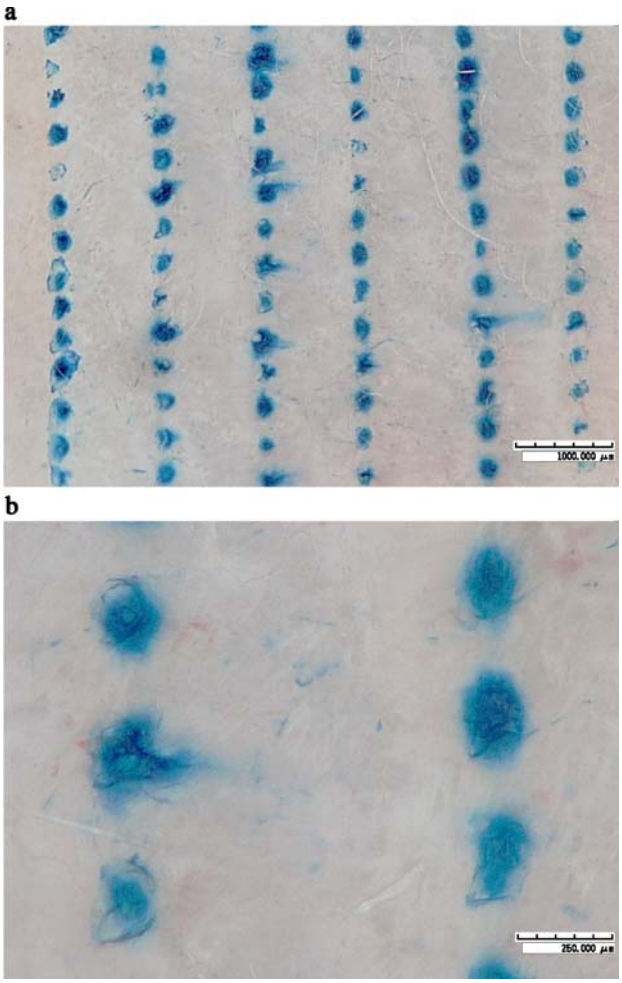

Fig. 3. Photographs of the hairless rat skin after the insertion of single layer 500 μm long microneedles and following application of methylene blue dye (**a**) and magnified view that shows diffusion of the dye along the periphery of microchannels (**b**).

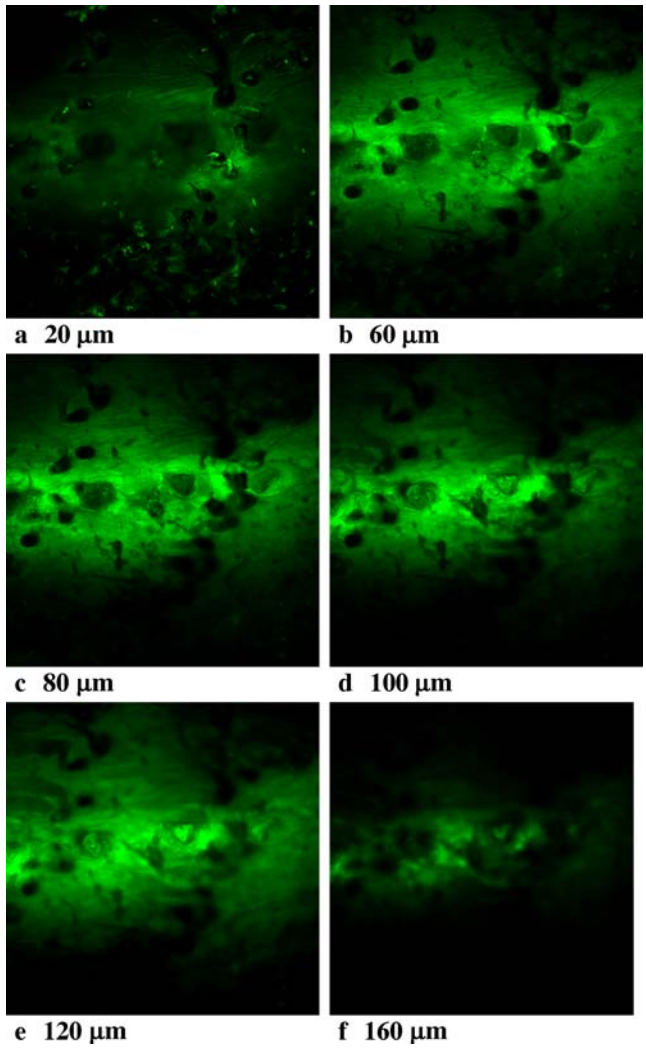

Fig. 4. a–f Confocal micrographs of permeation pathways of calcein across hairless rat skin at varying depths from the surface. Calcein is transported down through the stratum corneum into the epidermal tissue through the microchannels (*bright areas*). *Dark areas* indicate lack of fluorescence. Hair follicles appear as *dark whorled structures* surrounding the microchannels and spiral through the epidermis.

Characterization of Pore Uniformity

Image analysis was carried out by Fluoropore software developed by Altea Therapeutics (Tucker, GA, USA). Briefly, the image collected (Fig. 6a) is processed basing on the bloom around the each pore, which is indicative of volumetric distribution of calcein for that particular pore (Fig. 6b). For each micropore, a single number, the Pore Permeability Index (PPI) was produced which was representative of the total amount of calcein present in relative terms. PPI values allow accurate, ratiometric comparisons of the flux enabled by each pore.

The PPI values computed following collection of the calcein exposed microneedle treated skin had a mean value of 2.3 with a standard deviation of 1.27 for all 79 pores. Four of the pores were assigned zero PPI values. A histogram,

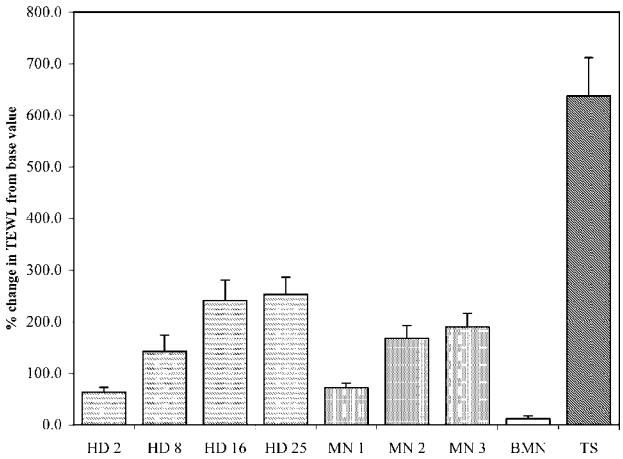

Fig. 5. Effect of microneedles, hypodermic needles (26 G) and tape stripping on transepidermal water loss (TEWL) of hairless rat skin measured as percentage change relative to the intact skin. Skin pricked 2 (HD 2), 8 (HD 8), 16 (HD 16) or 25 (HD 25) times using hypodermic needle, skin treated with just the base with no microneedles (BMN), single (MN 1), two (MN 2) or three (MN 3) arrays microneedles and following tape stripping (TS) was compared to normal skin. Sites treated with hypodermic needles, microneedles and tape stripped skin showed a significantly greater value as compared to base value ($P < 0.05$).

shown in Fig. 6c, with all the PPI values shows a relatively narrow distribution centered about PPI of 2.3, which is indicative of uniformly created pores.

Microneedle Mediated *In Vitro* Transdermal Delivery of NH

When inserted into the hairless rat skin, microneedle arrays increased transdermal permeation of NH. Figure 7 shows the cumulative amount of NH permeated with time. Curve with solid rectangles represents NH transport through rat skin in the presence of single array of 500 μm microneedles. Curve with hollow triangles represents passive delivery of NH in the absence of microneedles and curve with solid triangles in the same figure represents delivery of NH through rat skin treated with the base of the microneedle array holder, which in the absence of microneedles, served as a pressure control for the experiments.

Passive diffusion of NH was low with a mean flux value of 1.72 μg/cm^2/h and pre-treatment with microneedles increased the mean flux value to 7.05 μg/cm^2/h while the flux value was 2.16 μg/cm^2/h for skin treated with the base of the microneedle array and without microneedles. Also, the lag time was reduced from 10.4 to 7.6 h after treatment with microneedles. The results indicate a statistically significant increase ($P < 0.05$) in the permeation of NH through skin following treatment with microneedles while no difference was observed between passive delivery and skin treated with base of the holder for microneedles.

In Vivo Studies

The enhanced transdermal delivery was also demonstrated *in vivo* in rats. Figure 8 shows the pharmacokinetic profiles of nicardipine in hairless rats for 24 h. It was shown that nicardipine plasma levels in hairless rats pretreated with maltose microneedles reached peak plasma levels (Cmax) of 56.45 ng/ml. In contrast, passive delivery was low and detectable levels could be seen only after 8 h. Area under the curve (AUC_{0-t}) for pretreatment (779.77 ng h/ml) was significantly greater as compared to that following passive delivery (211.22 ng h/ml).

DISCUSSION

Microneedle technology promises to expand the scope of transdermal delivery by allowing the transport of therapeutic agents of any size across the skin and the development of biocompatible and biodegradable microneedles is an advance in this field. Our study presents use of microneedles fabricated out of maltose utilizing micromoulding technology. In-plane solid maltose microneedles have the advantage of better control over the design as the lithography of the micromould lies in the same plane. Unlike few other in-plane microneedles these can be stacked easily as per requirement. Also, microneedles of different lengths can be fabricated for specific purposes and this allow controlled delivery of therapeutic agents to specific regions or target sites in the skin.

In order to be minimally invasive, the needles should be small and designed to be very sharp. Tip radius of 3 μm for maltose microneedles is reasonably sharp enough to allow the needles to be easily and effectively inserted into the skin. In addition, the small size of the needles causes less compression of the tissue. The imposed local high strain to the stratum corneum by the sharp micron sized needles appears to be responsible for the loss of barrier integrity of corneocytes and the intercellular lipid multilayers. Also, as seen from Fig. 2, the surface morphology of the hole created in the treated skin was noticeably close to the shape of the microneedle. The microchannels measured about 55.42 ± 8.66 μm at their widest opening. Though the needles measure 500 μm in length, the effective penetration would be much lower for two obvious reasons, first because, once the maltose microneedle penetrates the stratum corneum and enters the underlying epidermal layer, it gets dissolved as it encounters environment where the water content can reach as high as 70% (14). The second reason being, as an initial contact of the microneedle is developed with the skin, pressure applied first indents because of elastic nature of the skin and only after a sufficient pressure is applied, penetration of the needle in to the skin occurs. So part of the needle just indents the skin while the rest penetrates. Our observation was consistent with earlier reports in the literature (15).

Methylene blue cannot be taken up by skin with intact stratum corneum but once the skin is compromised by pretreatment with microneedles, integrity of stratum corneum is broken and methylene blue diffuses through these compromised areas of the skin. However, impressions caused by base of microneedle or the adjacent areas did not take up methylene blue and this reveals that there was no damage caused to the skin due to the base of the microneedle holder.

Laser scanning confocal microscopy can be used to obtain horizontal and vertical optical sections in thick samples without fixing or cutting the specimen and thus it is possible to prepare and examine fresh skin samples without fixation artifacts or distortion. It was earlier used to visualize the pathways of permeation taken by iontophoretically driven fluorescent probes (16) and Cevc has used confocal

microscopy to demonstrate that his mixed vesicle systems penetrated intact through the skin (17).

The transport of low molecular weight fluorescent marker, calcein, appears to take place primarily through microchannels created by microneedles (Fig 4a–f). Fluorescence beneath the stratum corneum is primarily due to calcein that has traveled down the stratum corneum through the microchannels. Fluorescence appeared up to a depth of 160 μm. It was not observed in the follicular shafts or appendages as seen in Fig. 4a indicating that calcein was not transported through follicular pathway or through the appendages. This also was evident from the Fig. 4e–h that show localization of the dye in the microchannels. Low intensity at a depth of 20 μm could be due to lack of ability of stratum corneum to take up calcein and also due to blotting of calcein from the surface of skin, which was essential to avoid excessive fluorescence. The decrease in intensity with increasing depth above 80 μm is due to scattering and absorbance within the skin and no fluorescence was observed at beyond a depth of 180 μm. Based on the above observations the depth of penetration into skin was estimated approximately to be about 160 μm. In humans, the stratum corneum is about 10–20 μm in thickness, with the underlying epidermis layer being about 150 μm thick (4). Therefore, this penetration depth should be sufficient breach the stratum corneum without stimulating nerves in deeper tissues. These confocal studies therefore demonstrate the localization of calcein in the areas in and around the microchannels and thus indicate that microneedles can create transport pathways for drug molecules.

Measurement of TEWL is a sensitive evaluation of the integrity of the stratum corneum (18). It allows discovering disturbances in the barrier nature of skin in an early stage, even before they are noticeable. Normal skin, in general allows water loss only in small amounts whereas the water

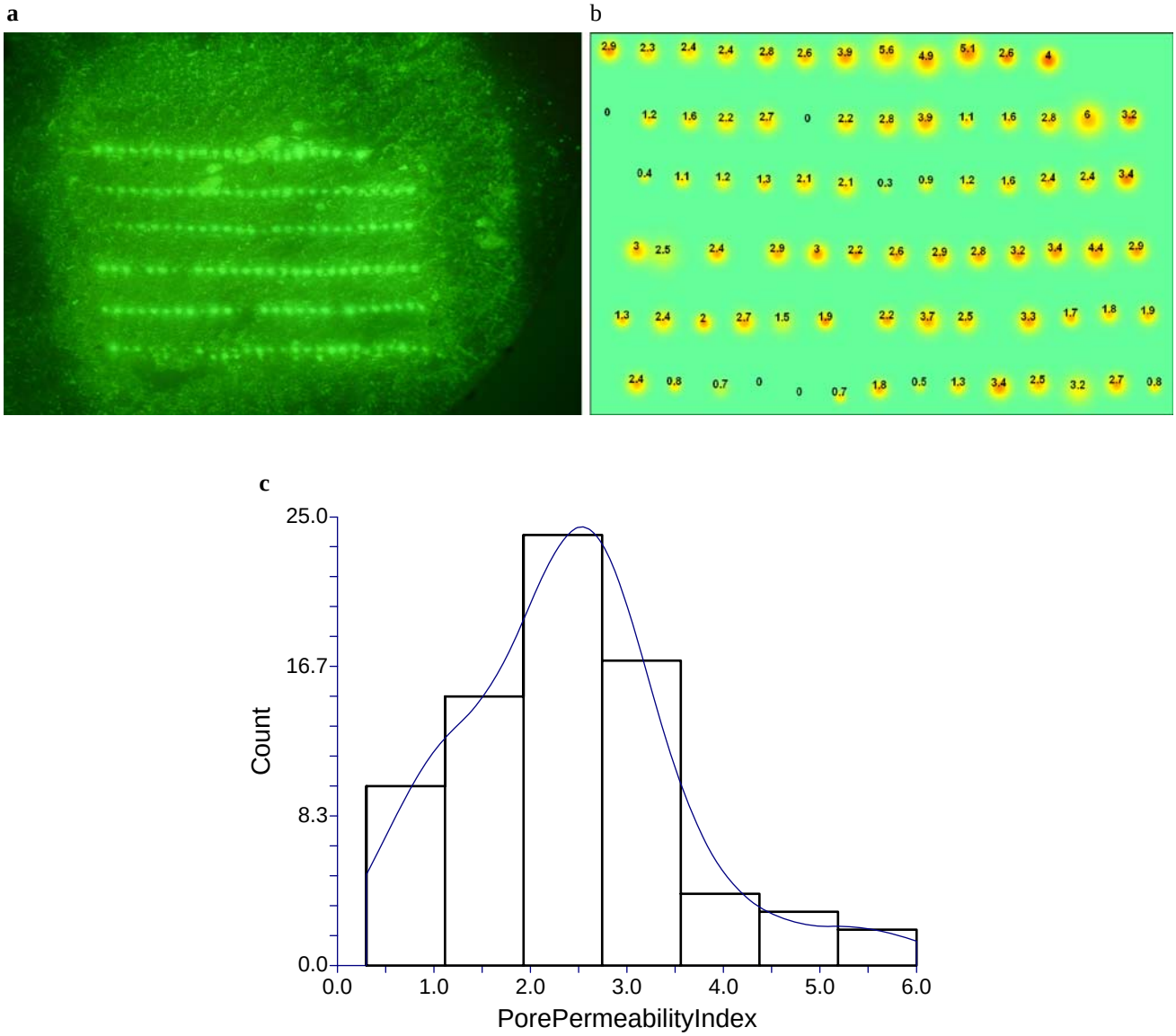

Fig. 6. **a** Microneedles treated skin exposed to calcein and after calibration correction, the initial location of pores are marked, bounding box is applied to each pore and high values are masked. Fitting in to software that computes the Pore Permeability Index (PPI) values and constructs an interpreted image 6 (**b**). Plot of histogram 6 (**d**) that shows PPI values associated with pores.

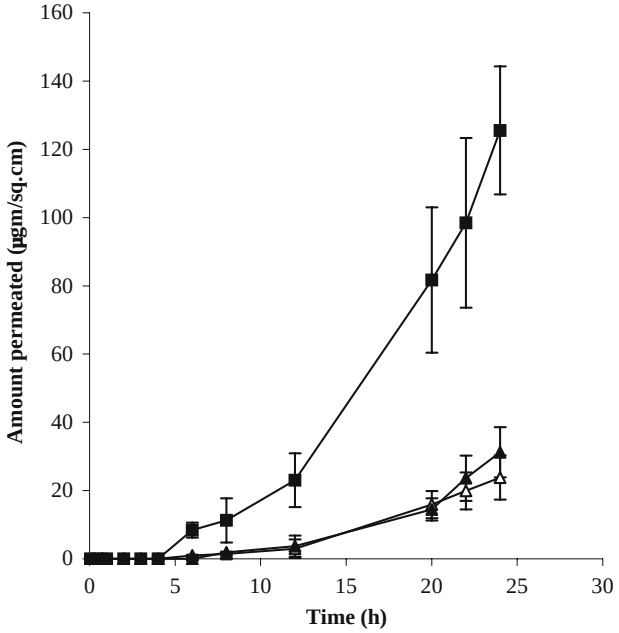

Fig. 7. *In vitro* transdermal delivery of nicardipine hydrochloride across hairless rat skin following treatment with 500 µm long single line maltose microneedle (*filled square*), treatment with base of the microneedle alone without microneedles (*filled triangle*) and passive diffusion as control (*open triangle*). Each value represents the mean ± SD of 3 experiments.

loss is higher for a compromised skin. The TEWL measurements are used as an important support to study the changes in barrier nature of the skin that occurs due to various physical and chemical influences. Also, this model is used to evaluate the integrity of isolated skin for *in vitro* experiments (19). Hairless rat skin samples treated with microneedles were identified by the TEWL data as exhibiting a compromised barrier function. Increased TEWL values following treatment with microneedles was indicative of barrier disruption, which was not seen, with base of the microneedle holder.

For hairless rat skin, a TEWL value of 5.9 g/m^2/h was observed as a base value under ambient room conditions. TEWL following treatment with either hypodermic needles or microneedles was well above this value (Fig. 5). Generally, chemicals or treatments that breach the skin barrier and increase permeability would cause a change in the TEWL. Though there was an increase in TEWL value indicating compromised skin, the value observed was not as high as seen with tape stripped skin (43.5 g/m^2/h). This probably may be due to relatively very small area of disruption (0.4%) caused by microneedles as compared to tape stripping. We have used hypodermic needles to create pores in the skin and our experiment demonstrates that pores created in skin results in increased TEWL values and similar phenomenon was observed with microneedles indicating that pores are created similar to those with hypodermic needles and with added advantage of being painless. This change in the TEWL increased by doubling the microneedle arrays but further increase resulted in no change, similar to that observed with hypodermic needles. Dye binding studies revealed no evidence of any damage caused to skin by means other than microneedles.

The results thus demonstrated the applicability of the TEWL measurements to identify the disruption caused in full-thickness skin treated with microneedles. Further confirmation of the ability of TEWL measurements to provide a more rapid assessment of barrier integrity was substantiated by results from confocal microscopic studies, visualization studies and *in vitro* penetration experiments.

In earlier experiments, we have established that maltose microneedles breach the skin and create the microchannels and we later made an effort to demonstrate that the micropores created have relatively uniform permeability. As mentioned in the confocal studies, calcein is not taken up by intact SC but can permeate through the areas where SC is breached. Moreover, calcein exhibits fluorescence and hence can be selectively visualized so this molecule was used for the characterization of pore uniformity.

Though the PPI values that were obtained following image collection and data processing depends on duration of exposure to calcein and length of microneedles, it gives relative values for a particular protocol and these are reproducible as observed from our experiments that were conducted in triplicate. Also, increased exposure times to calcein lead to blooming of the pores with the consequence that adjacent pores got merged, resulting in isolation of pores being difficult. Further, the pores in the skin are spaced narrow with the microneedle design so an attempt to increase exposure time might result in overlapping of the pores and therefore a short exposure time of 1 min was selected. As illustrated in Fig. 6c, values show a relatively narrow distribution centered about PPI of 2.3 and indicates uniform uptake by the pores.

Overall, it can be concluded from this experiment that microchannels created upon treatment with microneedles in hairless rat skin uptake calcein rather uniformly for a particular treatment. The speed and efficiency of this method makes it a valuable tool for quantifying permeability through micropores created in the skin.

The relative increase in NH transport across the skin is a consequence of physical disruption of stratum corneum

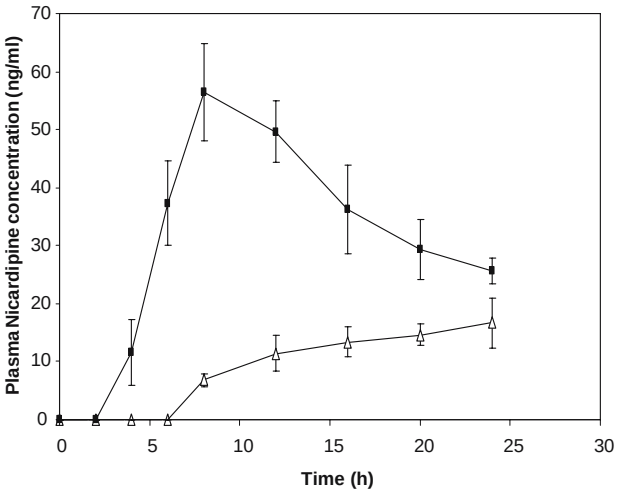

Fig. 8. Plasma levels of nicardipine following *in vivo* transdermal delivery in hairless rats pretreated with six 500 µm long maltose microneedles (*filled square*), and passive diffusion as control (*open triangle*). Each value represents the mean ± SD of 3 experiments.

caused by microneedles resulting in decreased barrier resistance and creation of new, additional and effective pathways for the transport. Results shows that NH did not permeate through skin just because of pressure applied on the microneedle arrays but the delivery was due to the microneedles causing microscopic channels for drug transport. The application and considerable potential of this technology for the cutaneous delivery of low molecular weight medicaments has been previously reported (20).

In vitro permeation study was conducted with single array of microneedles that would create 27 microchannels for drug transport and flux of NH per pore was calculated to be 0.26 μg/cm^2/h. When extrapolated to sq. cm area, 250 microchannels would be created resulting in overall flux of 65 μg/cm^2/h. NH has a plasma clearance of 0.4 L/h kg (21) and based on this and flux from our *in vitro* studies, the patch size required to deliver the required dose for a 70 kg adult can be calculated using (22):

$$J_{\text{Skin}} \times \text{SA} = C_{\text{SS}} \times \text{Cl}_T$$

Where J is the flux, C_{ss} is steady state concentration and Cl_T is the total clearance. It was calculated that a patch of 15.5 sq cm would be required to achieve the desired level of 36 ng/ml (23). The limitation of this calculation is that projections are based on hairless rat skin data. This should be achievable by transdermal delivery and our *in vivo* studies in hairless rats (Fig. 8) showed greater Cmax levels and decreased lag time following pretreatment with microneedles as compared to passive delivery.

Maltose microneedles were also shown to enhance delivery of NH *in vivo* though the enhancement was not as high as seen with *in vitro*. One possible reason might be due to the cushioning effect of underlying fat and subcutaneous tissue reducing the efficacy of penetration of the microneedles. Lag time was lower *in vivo* compared to *in vitro* and this might be because during *in vitro* experiments, relatively hydrophobic NH has to traverse through out the entire thickness of the skin before it reaches the receptor compartment whereas drug is immediately picked by the microcirculation when it crosses the epidermis *in vivo*. Our observations were consistent with those seen by Sintov *et al.* (20) who delivered therapeutic molecules *in vitro* and *in vivo* through microchannels created in skin using radio frequency ablation.

The diameter of microchannel created by microneedle is about 55 μm and this would disrupt an area of 1,590 square microns, which would be around 0.4% of the total exposed area. Therefore, due to small area of exposure, even when other enhancement techniques like iontophoresis, are used in conjunction, the skin might retain its permselective characteristics. In addition, low depth of penetration and use of a GRAS substance (maltose) for the manufacture of microneedles may render them safe and nonirritant to use.

CONCLUSIONS

Microneedles have been demonstrated earlier as useful drug delivery system for the delivery of therapeutic molecules to target regions in the skin and systemically. Solid in-plane maltose microneedle, about 500 μm tall, were characterized and studied for possible transdermal application. They were inserted manually into the skin and upon insertion they dissolved and disappeared rapidly while creating microconduits for drug transport. With sharp radius of curvature of the tip of about 3 μm, they effectively breached the stratum corneum and allowed direct access to the underlying epidermis. They can be stacked uniformly to obtain and desired pore density and low penetration depth of around 160 μm, as measured by confocal studies, makes them minimally invasive and painless. Calcein, used as a marker, was demonstrated to have followed the microchannels for its transit across the skin. Through independent experiments we have demonstrated that treatment using maltose microneedles increase the permeability of the skin as assessed by TEWL values and uptake of the marker molecule was relatively uniform by the individual pores. Increased *in vitro* and *in vivo* transdermal delivery was observed for nicardipine hydrochloride following treatment with microneedles and results demonstrate that several folds increase in flux could be attained with appropriate microneedle design. Overall, these studies demonstrate that maltose microneedles can serve the purpose of disrupting the stratum corneum to increase the drug transport across the skin.

ACKNOWLEDGEMENTS

Microneedles required for the study were developed and supplied by Texmac Inc. We thank Dr. Lisa Hoskin and Gautam Patel (Georgia Tech Research Institute, Atlanta, GA) for their help with SEM and Videomicroscope images; Janice Taylor, University of Nebraska Medical center (Omaha, NE) for help with confocal microscopy and David Farquhar, Altea Therapeutics (Tucker, GA), for help in image processing.

REFERENCES

1. M. Kendall. Engineering of needle-free physical methods to target epidermal cells for DNA vaccination. *Vaccine* **24**:4651–4656 (2006).
2. S. Coulman, C. Allender, and J. Birchall. Microneedles and other physical methods for overcoming the stratum corneum barrier for cutaneous gene therapy. *Crit. Rev. Ther. Drug Carr. Syst.* **23**:205–258 (2006).
3. A. K. Banga. New technologies to allow transdermal delivery of therapeutic proteins and small water-soluble drugs. *Am. J. Drug Deliv.* **4**:221–230 (2006).
4. S. Henry, D. V. McAllister, M. G. Allen, and M. R. Prausnitz. Microfabricated microneedles: a novel approach to transdermal drug delivery. *J. Pharm. Sci.* **87**:922–925 (1998).
5. A. L. Teo, C. Shearwood, K. C. Ng, L. Jia, and S. Moochhala. Transdermal microneedles for drug delivery applications. *Mater. Sci. Eng. B* **132**:155–158 (2006).
6. Y. Ito, E. Hagiwara, A. Saeki, N. Sugioka, and K. Takada. Feasibility of microneedles for percutaneous absorption of insulin. *Eur. J. Pharm. Sci.* **29**:82–88 (2006).
7. S. C. Kuo and Y. Chou. A novel polymer microneedle arrays and PDMS micromolding technique. *Tamkang J. Sci. Eng.* **7**:95–98 (2004).
8. J. H. Park, M. G. Allen, and M. R. Prausnitz. Biodegradable polymer microneedles: fabrication, mechanics and transdermal drug delivery. *J. Control. Release* **104**:51–66 (2005).
9. C. M. Fernandes, V. M. Teresa, and F. J. Veiga. Physicochemical characterization and *in vitro* dissolution behavior of nicardipine-cyclodextrins inclusion compounds. *Eur. J. Pharm. Sci.* **15**:79–88 (2002).

10. E. M. Sorkin and S. P. Clissold. Nicardipine. A review of its pharmacodynamic and pharmacokinetic properties, and therapeutic efficacy, in the treatment of angina pectoris, hypertension and related cardiovascular disorders. *Drugs* **33**:296–345 (1987).
11. I. Diez, H. Colom, J. Moreno, R. Obach, C. Peraire, and J. Domenech. A comparative *in vitro* study of transdermal absorption of a series of calcium channel antagonists. *J. Pharm. Sci.* **80**:931–934 (1991).
12. T. Miyano, Y. Tobinaga, T. Kanno, Y. Matsuzaki, H. Takeda, M. Wakui, and K. Hanada. Sugar micro needles as transdermic drug delivery system. *Biomed. Microdevices.* **7**:185–188 (2005).
13. J. Pinnagoda, R.A. Tupker, T. Agner, and J. Serup. Guidelines for transepidermal water loss (TEWL) measurement. A report from the Standardization Group of the European Society of Contact Dermatitis. *Contact Dermatitis* **22**:164–178 (1990).
14. P. J. Caspers, G. W. Lucassen, H. A. Bruining, and G. J. Puppels. Automated depth-scanning confocal Raman microspectrometer for rapid *in vivo* determination of water concentration profiles in human skin. *J. Raman Spectrosc.* **31**:813–818 (2000).
15. W. Martanto, J. S. Moore, T. Couse, and M. R. Prausnitz. Mechanism of fluid infusion during microneedle insertion and retraction. *J. Control. Release* **112**:357–361 (2006).
16. N. G. Turner and R. H. Guy. Visualization and quantitation of iontophoretic pathways using confocal microscopy. *J. Investig. Dermatol. Symp. Proc.* **3**:136–142 (1998).
17. G. Cevc and G. Blume. Lipid vesicles penetrate into intact skin owing to the transdermal osmotic gradients and hydration force. *Biochim. Biophys. Acta* **1104**:226–232 (1992).
18. K. V. Roskos and R. H. Guy. Assessment of skin barrier function using transepidermal water loss: effect of age. *Pharm. Res.* **6**:949–953 (1989).
19. F. Benech-Kieffer, P. Wegrich, and H. Schaefer. Transepidermal water loss as an integrity test for skin barrier function *in vitro*: assay standardization. In K. R. Brain, V. J. James, and K. A. Walters (eds.), *Perspectives in Percutaneous Penetration*, STS, Cardiff, (1997), p. 56.
20. A. C. Sintov, I. Krymberk, D. Daniel, T. Hannan, Z. Sohn, and G. Levin. Radiofrequency-driven skin microchanneling as a new way for electrically assisted transdermal delivery of hydrophilic drugs. *J. Control. Release* **89**:311–320 (2003).
21. Cardene (nicardipine hydrochloride) injection; http://dailymed.nlm.nih.gov/dailymed/fdaDrugXsl.cfm?id=3820&type=display (Accessed 4-25-2007).
22. R. Panchagnula, R. Bokalial, P. Sharma, and S. Khandavilli. Transdermal delivery of naloxone: skin permeation, pharmacokinetic, irritancy and stability studies. *Int. J. Pharm.* **293**:213–223 (2005).
23. Nicardipine Hydrochloride capsule [GENPHARM INC.]; http://dailymed.nlm.nih.gov/dailymed/drugInfo.cfm?id=2762 (Accessed 05-05-07).